Crocetin delays brain and body aging by increasing cellular energy levels and enhances the median life span in aged C57BL/6J mice

Sushil Choudhary[1], Vishnu Kumar[2], Kuhu Sharma[3], Abhishek Gour[3], Ashish Sahrawat[4], Anshika Jotshi[3], Diksha Manhas[3], Utpal Nandi[3], Sandip Bharate[5], Zabeer Ahmed[6], and Ajay Kumar[3]

[1]CSIR Indian Institute of Integrative Medicine
[2]Justus Liebig University Giessen Institute of Anatomy and Cell Biology
[3]Indian Institute of Integrative Medicine CSIR
[4]Indian Institute of Science
[5]Indian Institute of Chemical Technology
[6]Council of Scientific & Industrial Research Indian Institute of Integrative Medicine

October 4, 2023

Abstract

Abstract Background and Purpose Aging is usually accompanied by mitochondrial dysfunction, reduced energy levels, and cell death in the brain and other tissues. Mitochondria play a crucial role in maintaining cellular energy through oxidative phosphorylation (OXPHOS). However, OXPHOS is impaired as mitochondrial oxygen supply decreases with age. We explored whether pharmacologically increased oxygen diffusion by crocetin can restore OXPHOS and help delay aging of brain and other vital organs. Experimental Approach Stress-free chronic treatment of aged C57BL/6J mice with crocetin followed by an analysis of behavior, hippocampi whole transcriptome, and key energy metabolites by LCMS was performed. Key Results The aged mice treated with crocetin for four months displayed significantly improved memory behavior, neuromuscular coordination, and ATP and NAD+ levels in the brain and other vital organs, leading to an increased median life span. The transcriptomic analysis of hippocampi from crocetin-treated mice revealed that enhanced brain energy level was caused by the upregulation of genes linked to OXPHOS, and their expression was close to the expression in young mice. The chronic treatment of aged astrocytes also showed improved mitochondrial membrane potential and energy state of the cells. Conclusion and Implications Our data suggest that restoring the OXPHOS and the normal energy state of the cell can delay aging and enhance longevity. Therefore, molecules like crocetin should further be explored to treat age-related diseases.

Crocetin delays brain and body aging by increasing cellular energy levels and enhances the median life span in aged C57BL/6J mice

Sushil Choudhary[1,2], Vishnu Kumar[3], Kuhu Sharma[1,2], Abhishek Gour[1,2], Ashish Sahrawat[4], Anshika Jotshi[1,2], Diksha Manhas[1,2], Utpal Nandi[1,2], Sandip B. Bharate[2,5], Zabeer Ahmed[1,2], Ajay Kumar[1,2*]

[1]Pharmacology Division, CSIR-Indian Institute of Integrative Medicine; Jammu, 180016, India.

[2]Academy of Scientific and Innovative Research; Ghaziabad, 201002, India.

[3]Institute of Anatomy and Cell Biology, Justus Liebig University of Giessen; Giessen, 35390, Germany.

[4]Molecular Biophysics Unit, Indian Institute of Science; Bengaluru, 560012, India.

[5]Natural Product and Medicinal Chemistry Division, CSIR-Indian Institute of Integrative Medicine; Jammu, 180016, India.

Email addresses of all authors

SC (sushil.choudhary24@gmail.com), VK (vcthakur42@gmail.com), KS (kuhu.sharma3141@gmail.com), AG (abhigour123@gmail.com), AJ (anshikajotshi@gmail.com), AS (ashishs1@iisc.ac.in), DM (dikshathakur771@gmail.com), UN (unandi@iiim.ac.in), SBB (sbharate@iict.res.in), ZA (zahmed@iiim.res.in), AK (ajaykumar@iiim.res.in)

*Correspondence

Ajay Kumar

ajaykumar@iiim.res.in

ajaykumar@iiim.ac.in

Running Title: Crocetin delays brain and body aging in aged mice

List of Abbreviations:

OXPHOS

Oxidative Phosphorylation

ETC

Electron Transport Chain

COPD

Chronic Obstructive Pulmonary Disorder

ODEs

Oxygen Diffusion Enhancers

TSC

Trans Sodium Crocetinate

PCA

Principal Component Analysis

LFC

Log 2-Fold Change

GO

Gene Ontology

KEGG

Kyoto Encyclopaedia of Genes and Genomes

BP

Biological Processes

MF

Molecular Function

CC

Cellular Components

GATK4

Genomic Analysis Toolkit 4

SNPs

Single-Nucleotide Polymorphisms

$\Delta\Psi\mu$

Mitochondrial Membrane Potential

MFI

Mean Fluorescence Intensity

RLT

Regularized Log Transformation

BQSR

Base Quality Score Recalibration

IGV

Integrative Genome Viewer

RIN

RNA Integrity Number

Abstract

Background and Purpose

Aging is usually accompanied by mitochondrial dysfunction, reduced energy levels, and cell death in the brain and other tissues. Mitochondria play a crucial role in maintaining cellular energy through oxidative phosphorylation (OXPHOS). However, OXPHOS is impaired as mitochondrial oxygen supply decreases with age. We explored whether pharmacologically increased oxygen diffusion by crocetin can restore OXPHOS and help delay aging of brain and other vital organs.

Experimental Approach

Stress-free chronic treatment of aged C57BL/6J mice with crocetin followed by an analysis of behavior, hippocampi whole transcriptome, and key energy metabolites by LCMS was performed.

Key Results

The aged mice treated with crocetin for four months displayed significantly improved memory behavior, neuromuscular coordination, and ATP and NAD+ levels in the brain and other vital organs, leading to an increased median life span. The transcriptomic analysis of hippocampi from crocetin-treated mice revealed that enhanced brain energy level was caused by the upregulation of genes linked to OXPHOS, and their expression was close to the expression in young mice. The chronic treatment of aged astrocytes also showed improved mitochondrial membrane potential and energy state of the cells.

Conclusion and Implications

Our data suggest that restoring the OXPHOS and the normal energy state of the cell can delay aging and enhance longevity. Therefore, molecules like crocetin should further be explored to treat age-related diseases.

Key Words

Crocetin; Brain Aging; Oxidative Phosphorylation; Oxygen; Electron Transport Chain

Introduction

Aging is an inevitable process characterized by a gradual decline in the physiological function of organs and increased vulnerability to death (Guo et al., 2022). The aging of the brain is strongly linked to the development of several neurodegenerative diseases (Fricker, Tolkovsky, Borutaite, Coleman & Brown, 2018; Gorman, 2008). In this context, targeting brain aging may present an opportunity to counter the development of age-related neurodegenerative diseases. Among several hallmarks of aging, brain aging and neurodegenerative diseases, mitochondrial dysfunction is one of the most significant factors (Mattson & Arumugam, 2018; Wilson, Cookson, Van Den Bosch, Zetterberg, Holtzman & Dewachter, 2023). Mitochondrial dysfunction plays a vital role in reducing the availability of energy metabolites in the brain and other organs of the body (Boveris & Navarro, 2008; Johri & Beal, 2012). The proper functioning of mitochondrial ETC requires a continuous supply of oxygen, which acts as a final acceptor of electrons (Johri & Beal, 2012; Mitchell, 1970; Wilkins & Swerdlow, 2021). However, its availability to the tissues is reduced significantly during aging due to various factors like reduced lung capacity, anemia, COPD, compromised microvascular network, and other age-related changes leading to hypoxia and mitochondrial dysfunction (Borson et al., 2008; Dodd, Getov & Jones, 2010; Hong et al., 2013; Lowery, Brubaker, Kuhlmann & Kovacs, 2013; Moeini et al., 2018; Snyder, Simone, Giovannetti & Floyd, 2021). Additionally, chronic hypoxia is a strong trigger for the development of neurodegenerative diseases (Li et al., 2022; Webster, Green, Settle, Peers & Vaughan, 2004), which can be reversed by oxygenation therapy (Arjun, Acharya, Shender, Rorres, Hrebien & Kam, 2019; Ferrari et al., 2017; Kim et al., 2013; Shapira et al., 2021). Therefore, to stop the development of pathological conditions, one of the possible ways to overcome the shortfall of oxygen may be to supplement the oxygen. Pharmacologically, a class of molecules called oxygen diffusion enhancers (ODEs) (Shah, Jain, Joshi & Kharkar, 2021) can be considered potential drug candidates to help overcome chronic hypoxia and related diseases. In this study, we used trans-crocetin's oxygen diffusion-enhancing property to restore ETC activity in aged mice and its effect on brain and body aging. Trans sodium crocetinate (TSC) is reported to alter the molecular arrangement of blood plasma's water molecules, creating a more ordered water structure (Stennett, Dempsey & Gainer, 2006). Oxygen diffuses faster in plasma with this altered water structure because of its low density. Thus, more oxygen can reach oxygen-deprived tissues, which has been proved in pre-clinical and clinical studies (Okonkwo et al., 2003) (NCT04808622). The oxygen-enhancing effect of TSC has been tested in several conditions responsible for low oxygen saturation, which include stroke (NCT03763929), hemorrhage shock (Wang, Schretter, Clarke & Lee, 2015; Wang et al., 2014), and high-altitude exercise (NCT05036980).

In this study, we investigated the efficacy of *trans-* crocetin to prevent or delay brain and body aging in 16-18 months old C57BL/6J mice. We treated the mice for four months and analyzed various parameters that could be affected by aging with a primary focus on the brain. This included memory behavior, hematology, biochemistry, and gene expression profile of hippocampi and analysis of energy metabolites (Supplementary Figure S2). We observed several interesting changes in the behavior and gene profile of the mice treated with crocetin, data of which are presented here.

Results

Chronic crocetin treatment of aged mice led to improvement in age-related deterioration of brain function

We treated aged mice for four months with crocetin to evaluate its effects on age-related cognitive behavior. However, for long-term treatment, we used a non-invasive and painless voluntary dosing method and trained the mice to take the drug as gelatin pellets containing crocetin (Supplementary video SV1). The uniformity of crocetin content in the gelatine-based formulation was confirmed by using RP-HPLC (Supplementary Table ST1).

Further, to confirm the penetration of crocetin into the brain while using a gelatin-based formulation, we performed an 8 h plasma and brain pharmacokinetic (pk) study with multiple points of oral dosing with 10 mg kg^{-1} of crocetin. Data revealed a significantly detectable quantity of crocetin is both plasma and the brain. (Figure 1A). Further, we found that after four months of treatment with crocetin, its level in the brain

was less than the levels observed during eight-hour pk studies, which ruled out any accumulation (Figure 1B). Additionally, we measured the mice's body weight at every 15 days during four months treatment and found no changes in the body weight (Supplementary Table ST2).

Further, the treated mice displayed significantly improved spatial memory, which was tested in an eight-armed radial arm maze. The animals treated with crocetin took a significantly less average time to search for their food reward as compared to the control group (Figure 1C). The treated animals also spent significantly longer time in the baited arm as compared to the control group (Figure 1C). Additionally, wrong entries into the non-baited arms were reduced to half in the crocetin group as compared to the untreated control group (Figure 1C). The crocetin group was also quick to find the baited arm, they travelled significantly less average distance in comparison to the control group (Figure 1C). Further, the crocetin group also displayed significantly improved working memory behavior in the radial arm maze, where alternate arms were baited. Improvement in the working memory was reflected in a number of tests that included improved latency to the first entry into the baited arm, where the crocetin group took less than half of the time than untreated group (Figure 1D). The Crocetin group also spent more average time in the baited arm as compared to the control group (Figure 1D). In contrast, the control group spent more time in the non-baited arms than the crocetin group (Figure 1D). The Crocetin group also showed a significantly higher number of entries into baited arms as compared to the control group (Figure 1D). The effect of crocetin was also observed clearly in the exploratory behavior of animals in the open field test. The Crocetin group spent more average time in the corners than the control group (Figure 1E). Crocetin treatment also improved the locomotor activity of mice, which were mobile for a significantly longer time (Figure 1E) and travelled significantly more distance (Figure 1E) at a higher speed (Figure 1E) while exploring the unfamiliar field as compared to the control group. The Crocetin group also displayed a significantly higher average number of rearing events as compared to the control group (Figure 1E), which appeared uninterested in exploring the unfamiliar environment. However, there was no significant difference in time spent in the centre between control and crocetin groups (Figure 1E).

Crocetin treatment differentially changed the expression of genes in the hippocampi of aged mice to bring about a change in memory behavior

To understand the molecular basis of changes observed in the memory behavior of treated mice, we isolated the hippocampi from the brain of mice and sequenced the whole transcriptome. To achieve greater accuracy in transcriptome sequencing, we used a depth of 40 million reads per sample. We conducted PCA analysis to compare the control and crocetin-treated groups. The results revealed significant insights into the variance and underlying patterns within the datasets. The initial nine principal components (PC1 to PC9) accounted for 84.06% of the total variance, suggesting potential treatment-related effects (Figure 2A & B). Further, differential gene expression analysis revealed that out of 22,096 protein-coding genes, 154 genes were differentially expressed (Figure 2C). A detailed differential gene expression list is provided as supplementary spreadsheet SS1.

We performed a hierarchical clustering to ensure to distinguish the upregulated and downregulated genes. We found a significant upregulation of Bdnf, Gabbr2, Gad2, and Drosha that correlated to the improved brain function and behavior of treated mice (Figure 2D and Supplementary Figure S3). Further, some of the genes downregulated after crocetin treatment could also be linked to improvement in brain function, these included Hck, Amigo3, Top1mt, and Lcp1 (Figure 2E).

Further analysis revealed that mitochondrial genes belonging to different complexes of ETC were significantly upregulated. The upregulated genes included ND1, ND2, ND4, ND4L, ND5, and ND6 related to NADH dehydrogenase from complex I, CYTB from complex III, Uqcrq from complex IV, and ATP6 and ATP8 from complex V (Figure 2F). Few more ETC genes, such as ND3, COX1, COX2, and COX3, were also found upregulated, though non-significantly (Supplementary Spreadsheet SS1).

Crocetin upregulated the electron transport chain to yield more energy in the brain of treated old mice

To identify the significant pathways affected by crocetin, we used the GO and KEGG pathway analysis (Supplementary Spreadsheet SS2). Most of the significantly upregulated pathways in the hippocampi of crocetin-treated mice were related to energy metabolism. GO dot plots depicting BP, MF, and CC identified energy metabolism pathways located in the mitochondria being the main target of crocetin. The BP related to the ETC were particularly found to be upregulated in crocetin-treated mice (Figure 3A). Further, CC analysis also showed high expression of genes belonging to various mitochondrial complexes involved in processing energy precursors (Figure 3A). The MF analysis further revealed the upregulated activity of mitochondrial membrane transporters and enzymes such as NADH dehydrogenase involved in the production of energy metabolites (Figure 3A). Additionally, the downregulated genes did not involve in any GO term at adjusted p value< 0.05.

KEGG pathway analysis of upregulated genes revealed oxidative phosphorylation as the main target of crocetin (Figure 3B). Thus, confirming the effect of crocetin on energy metabolism in the hippocampi. Similar to GO analysis, there were no pathways found to be downregulated in KEGG pathway analysis at adjusted p value< 0.05.

We further compared the levels of different energy metabolites in the whole brain samples of control and crocetin groups. The average NAD^+ levels were found to be about 50% higher in mice treated with crocetin than in the control group (Figure 3C). However, no significant change was observed in the levels of NADH between the two groups (Figure 3C). The ATP levels in the crocetin group were almost two times higher than the control group, though the levels of AMP were not changed significantly (Figure 3C). Further to know if the increased levels of NAD^+ and ATP were due to higher levels of glucose present in the brain, we analyzed its level in the brain through LCMS. Interestingly, crocetin-treated mice had two times higher concentrations of glucose in the brain than the untreated control group (Figure 3C). However, no increase in the plasma glucose level in the crocetin treated group was observed compared to the control group (Supplementary Table ST3).

Further to know if crocetin impact on the mitochondrial genome stability to cause its anti-aging effect, we compared the mitochondrial genome of old control mice with the crocetin group for the possible change in SNPs or InDels by using the GATK4 pipeline. However, our data showed that crocetin treatment did not alter the type of SNPs or InDels usually found in the aged mitochondrial genome (Supplementary Table ST4).

Crocetin restored the expression of multiple genes in the hippocampi of old mice to bring it closer to young mice

To know whether crocetin can restore the expression of hippocampi genes of old mice to the levels of young mice; we compared the gene expression profile of crocetin, control (untreated aged), and young mice groups. The hippocampi transcriptome data of young mice were taken from GEO NCBI (GSE147842) (Haghani et al., 2020).

The cluster dendrogram revealed three gene clusters viz. crocetin, aged control, and young mice. Wherein, crocetin cluster was closer to young mice as compared to aged mice, indicating the prevention of brain aging in crocetin group (Figure 4A). DSeq2 analysis revealed that most of the mitochondrial genome encoded ETC genes ND1, ND2, ND4, ND5, ND6, CYTB, COX1, and COX3 were significantly downregulated in aged hippocampi compared to young mice (Figure 4B). Further, crocetin treatment of aged mice clearly showed a significant improvement in the expression of these genes (Figure 4B). Interestingly, the expression of the genes Bdnf, Gabbr2, Gad2, Gfpt1, Drosha, and Uqcrq were found to have significantly high expression in young and crocetin treated group in comparison to untreated control mice (Figure 4B and Supplementary Spreadsheet SS3). We also confirmed the upregulation of two essential genes, ND5 and ND6 of ETC through western blotting, which confirmed our findings of functional upregulation of ETC (Figure 4C).

Crocetin restored the ETC function of mitochondria in aged primary astrocytes

We further assessed the functionality of mitochondrion in aged primary astrocytes (4^{th} passage) after treating

them for 15 days with crocetin at 25 μM (Wani et al., 2021). The flow cytometric analysis of mitochondrial membrane potential ($\Delta\Psi$m) revealed a significantly increased number of cells having higher Mito Tracker (CMXRos) fluorescence in crocetin treated cells than control samples indicating higher $\Delta\Psi$m (Figure 5A). We reconfirmed these findings by using confocal microscopy under similar experimental conditions. Here, we measured the mean fluorescence intensity (MFI) of individual mitochondria in each cell. There was a significant increase of Mito Tracker (CMXRos) MFI in crocetin-treated astrocytes in comparison to untreated control cells, however, there was no change in number and area of mitochondria between the samples (Figure 5B and Supplementary Figures S4A-D). Further analysis for the expression of mitochondrial inner membrane proteins ND5 and ND6 revealed that cells treated with crocetin had a significantly higher expression of these proteins than untreated aged astrocytes (Figure 5C). Furthermore, the aged astrocytes treated with crocetin also showed same pattern of change in the levels of NAD^+ and ATP as we found in the mice brain, though, there was no change in NADH and AMP levels between control and treated astrocytes (Figure 5D).

Crocetin upregulated the energy levels of other vital organs of the body and enhanced the median life span of male mice

After analyzing the anti-aging effect of crocetin on brain, we wanted to know if chronic treatment with crocetin had a similar effect on the energy metabolism of other vital organs including heart, kidney, lungs, and liver. All the organs showed similarly increasing trend in the levels of ATP, NAD^+ in crocetin group, and as expected, their level was closer to the levels in young mice (Figure 6A-D). Interestingly, NADH and AMP also showed higher levels in crocetin group than control group, indicating higher rate of metabolism in these organs (6A-D). Further, no significant change was observed in biochemical parameters including oral glucose tolerance test (OGTT) between the groups. The hematological parameters were not changed significantly except for a significant decrease in the platelet count in the crocetin group (Figure 6E and Supplementary Table ST3). The overall increased energy levels in different organs of mice body were also reflected in improved neuromuscular co-ordination in crocetin treated mice in comparison to untreated group as analyzed in the rotarod test. The crocetin group ride the rota road for a significantly longer average time as compared to the control group (Figure 6F). Additional proof of anti-aging effect of crocetin came from the increased grip strength of mice in the wire-hanging test, where crocetin-treated mice kept hanging for a significantly longer time in comparison to the control group (Figure 6G).

We further asked if improved energy levels of different orans of the body can increase the life span of the male mice. Therefore, after finishing the treatment, we observed the control and crocetin groups till the death of all the animals. We found that the median survival time of crocetin treated mice was significant improved by 17.7% from 744 days to 876 days (p value = 0.0024) (Figure 6H).

Discussion

Aging is usually accompanied by low levels of energy and frailty. In all the aerobic organisms' mitochondria are the main source of energy production. For generation of energy, they rely on the availability of oxygen. However, with age, due to various reasons, including reduced lung capacity, hematocrit, cardiac output, and capillary density the oxygen supply to the brain and other organs of the body gets considerably reduced (Ances et al., 2009; Moeini et al., 2018). Low oxygen levels further contribute significantly to mitochondrial dysfunction and aging. Although all the organs get stressed due to low oxygen availability, but brain is most prone to its adverse effects. Some PET scan-based studies have conclusively shown that the cerebral metabolic rate of oxygen (CMRO2) is significantly reduced in the aged brain tissue due to reduced oxygen availability (Goyal et al., 2017). Therefore, in this study, we asked whether we can delay the process of brain aging by pharmacologically increasing the availability of oxygen to the brain. Though, we also analyzed its effect on other vital orans of the body as well.

We used crocetin, a known oxygen diffusion enhancer to treat aged mice and analyze its effect on delaying brain aging. The mice treated for four months with crocetin did not show any stress and toxicity, which was evident by no adverse changes in the behavior, body weight, blood biochemistry and hematological parameters. The analysis of cognitive behavior indicated a highly significant shift in the crocetin group from

the normally aged untreated mice. Crocetin-treated mice showed significant improvement in both working and spatial memory behavior, apart from performing well in the exploratory behavior.

We further wanted to explore the molecular changes behind the improvement in memory and exploratory behavior. Hippocampus is one of the most important regions of the brain responsible for processing and storage of long-term memory, though its involvement in short-term memory is also being revealed (Hannula, Tranel & Cohen, 2006). Therefore, we performed the whole transcriptome analysis of hippocampi to identify the differential change in the gene expression after crocetin treatment. Transcriptome analysis clearly revealed that multiple genes were differentially expressed in the hippocampi of the crocetin group, which was correlated with behavior data and other parameters. These data further emphasized to explore the exact genes that may be responsible for changes in memory behavior. We found that some of the most significantly affected genes in crocetin-treated mice belong to the mitochondrial genome. Out of the 13 protein-coding genes of the mitochondrial genome, nine genes were significantly upregulated, which included ND1, ND2, ND4, ND4L, ND5, ND6, CYTB, ATP6, and ATP8. These genes play an important role in the ETC and hence contribute to the production of energy and affect the energy state of the cell. Interestingly, during aging, the subunits of OXPHOS encoded by the mitochondrial genome are specifically downregulated rather than the subunits encoded by the nuclear genome (Gomes et al., 2013). However, we found that the nuclear gene ubiquinol cytochrome c reductase (Uqcrq), which is a part of complex III of ETC, was also significantly upregulated in crocetin-treated mice. Moreover, we found that most of the pathways affected by crocetin belong to energy metabolism indicating its strong effect on OXPHOS. Interestingly, OXPHOS is the main target of most of the life span extension interventions (Tyshkovskiy et al., 2019). Crocetin also appeared to reverse brain aging by upregulating the OXPHOS. The highly significant increase in NAD^+ and ATP levels in the brain of crocetin-treated mice also supported these data. We also observed a significant rise in glucose levels in the brain, indicating that increased availability of oxygen by crocetin helped mitochondrial to produce energy more efficiently from glucose and helped restoring the glucose stores in the brain. This observation is important as mitochondrial dysfunction during neurodegeneration is linked to less efficient glucose metabolism by glycolysis (Yao, Irwin, Zhao, Nilsen, Hamilton & Brinton, 2009).

We hypothesized that the ability of crocetin to enhance the diffusion of oxygen to the tissues might be contributing to the increased expression of ETC genes and the generation of more NAD^+ and ATP. Due to the high demand of energy, neurons have a large number of mitochondria, which require continuous supply of oxygen to produce ATP (Oruganty-Das, Ng, Udagawa, Goh & Richter, 2012). Our data indicated that treatment with crocetin helped the old brain cells to meet the demand of oxygen and regain the mitochondrial activity that could sustain different cellular functions. The declining level of NAD^+ have been reported to create hypoxia-like conditions in the cells, which show altered metabolic activities. Further, these conditions may not be reversible even if the oxygen is present in abundance (Gomes et al., 2013). However, we found that increased availability of oxygen by chronic treatment with crocetin restored the mitochondrial activity and production of energy metabolites NAD^+ and ATP in the brain cells. Further, few SNPs and InDels in mitochondrial have been linked with mitochondrial dysfunction and development of aging (Park & Larsson, 2011). However, we did not find any change in the pattern of SNPs and InDels, which further supported the increased availability of oxygen as a primary cause for improved mitochondrial function in the animals treated with crocetin.

Further, we compared the hippocampi gene expression profile of young mice with old and crocetin-treated mice. In cluster diagram, we found that the gene expression profile of young mice is closer to crocetin-treated mice. Additionally, the expression of mitochondrial genes was significantly high in young mice in comparison to old mice, however, crocetin treatment of old mice narrowed down this difference. These findings were also confirmed by the western blotting of two of the key protein ND5 and ND6, from NADH dehydrogenase complex I of ETC. These data further emphasized the anti-brain aging effect of crocetin. Additionally, a few important genes such as Bdnf, Gabbr2, Gad2, and Drosha that play a vital role in neuronal survival, growth, plasticity and neurotransmission (Podyma, Parekh, Guler & Deppmann, 2021), often show declining expression with aging (Kronenberg et al., 2021). However, we found that the expression of these genes was significantly upregulated in crocetin-treated mice, which was significantly closer to young than old mice.

The transcriptome data and the analysis of selective proteins clearly implicated mitochondria as the main target of crocetin. The reduction in the mitochondrial potential is a clear indicator of reduced mitochondrial activity and, thus production of energy, which is one of the hallmarks of aging (Leuner et al., 2007). Therefore, we intended to capture the effect of crocetin on the activity of mitochondria in aged primary astrocytes in the live cell assay for mitochondrial membrane potential. Being abundantly present in the brain, astrocytes contribute significantly to preserve physiological homeostasis in the brain (Khakh & Sofroniew, 2015; Verkhratsky & Nedergaard, 2018). We found that crocetin exerted its effect on a specific population of cells, among others, which had relatively low mitochondrial potential. The raised mitochondrial potential of these cells in the presence of crocetin also reflected in increased energy levels of the aged astrocytes. These data again emphasized the anti-brain aging effect of crocetin that comes through the improved function of mitochondria in aged cells or animals.

The anti-aging effect of crocetin was not confined to brain only, the analysis of energy metabolites in other vital organs viz. lungs, liver, heart and kidney of the mice treated with crocetin also showed significantly higher levels of ATP and NAD^+. These data clearly indicated that increased availability of oxygen affected the energy production pathways similarly across all tissues of the body. These data were further supported by improved neuromuscular co-ordination and muscular strength in mice treated with crocetin. Moreover, crocetin mediated improvement in energy metabolism through increased availability of oxygen also enhanced the median life span of mice. Our findings support the Tromsø study, which indicates that normal oxygen saturation levels are strongly linked to longevity (Vold, Aasebo, Wilsgaard & Melbye, 2015).

In conclusion, this study finds crocetin to be a potential lead molecule against brain and body aging. Crocetin prevents aging and increased median life span possibly by a unique mechanism of enhancing oxygen diffusion to the tissues. The increased oxygen helped rescue mitochondrial dysfunction, improve ETC activity and production of energy. Our data suggest that similar to calorie restriction, energy restoration can also have an anti-aging and longevity-enhancing effects. We believe that crocetin is worth exploring further for the possible development as a new drug against the neurodegenerative and other age-related diseases.

Materials and Methods

Chemicals, reagents, antibodies and other materials

The source of chemicals, reagents, antibodies and other resources is given in Table-1. The crocetin used in this study was synthesized and characterized in our lab (Reddy, Bharate, Vishwakarma & Bharate, 2020) (Supplementary Figure S1). Here, we have used the term crocetin instead of trans-croceitn, which constitutes 98% of the cis and trans mixture of crocetin.

Animal Care and Handling

This study used 16–18 months old C57BL/6J mice. The mice were housed in a temperature (22 ± 1°C) and humidity (40-60%) controlled room with a 12-h light/dark cycle and provided food and water ad libitum. Every 15 days, a proper record of their body weight and physical wellness was maintained during the study. Animals were randomized on the basis of their body weight. At the end of experiments, wherever required, animals were sacrificed by using CO_2 Inhalation method. All experiments were conducted after the approval of the institutional animal ethics committee.

Training and administration of the drug

The animals were trained to take the gelatin jelly voluntarily with vehicle jelly pellets (10% gelatine, 1% sucralose). Most of the animals (80%) liked the jelly and were trained for 15 days (Supplementary Video SV1). Every third day, all the jelly pellets (10% gelatine, 1% sucralose, and 25 mg ml^{-1} crocetin) were prepared and stored at 4 °C, and were given to mice daily except Sundays based on their body weight. All of the animals were kept under observation until they finished their dosing pellets, with the majority of them finishing in less than a minute.

Plasma and Brain pharmacokinetics studies of crocetin

The plasma and brain pharmacokinetics studies were carried out at 10 mg kg^{-1} (p.o.). Crocetin was given in the form of a liquid formulation similar to the one used during the treatment of animals for other studies. The formulation contained 10% gelatine, 1% sucralose and 25 mg ml^{-1} of crocetin. The formulation was kept at 37 °C to maintain its fluidity and administered orally via cannula at a concentration of 10 mg kg^{-1} of crocetin. Bood and Brain samples were taken at six different time points for up to 8 h of study. The quantitative analysis of crocetin present in blood plasma and brain was done by using LC-MS/MS method. The analysis of pharmacokinetic parameters was done by using PK solution software, Summit Research Services, USA.

Biochemical and hematological analysis of blood

For hematological and biochemical analysis, blood samples were collected from 8 animals from each group after 6 hours of fasting. Hematological parameters were examined by using automated hematology analyzer (XT1800i, Sysmex, USA). Serum biochemistry parameters were determined by using an automated clinical chemistry analyzer (EM360, Erba Mannheim group, Germany). Data were analysed through two-tailed student t-test.

Oral glucose tolerance test

OGTT was performed after overnight of fasting the animals. 1g kg^{-1} glucose solution was administered orally and blood glucose was recorded before and after glucose administration at different timepoints i.e., 15, 30, 60, 120 minutes using The Accu-Chek Active blood glucose meter (Roche).

Open-field test

The mice were acclimatized to the testing room for 30 minutes before the experiment. The open field arena box (60 cm x 45 cm x 25 cm) made up of white colored plastic was used for all the open field experiments. Individual mice were placed in the centre of the open field arena and were allowed to freely explore it for 5 minutes. The behavior of mice was recorded using a video camera connected to AnyMaze software. The following behavioral parameters were recorded: Total distance travelled (cm), average speed (m s^{-1}), time spent in the centre area (sec), time spent in the corners (sec) and the number of rearing events (counted manually after analyzing the recorded videos).

Working and spatial memory test in a radial-arm maze task

The eight-armed radial arm maze from UGO Basile was used to test working and spatial memory. The mice were acclimatized to the maze for three days before the experiment. For testing the spatial and the working memory, separate set of mice were used. Each mouse was trained to navigate the maze for three consecutive days. The mouse was placed on the end of one arm (entry arm). For working memory, a food reward (100 mg of chocolate cookies) was placed at the end of four randomly selected arms. The movement of mice was tracked with the help of automated AnyMaze software connected with a tracking camera. A choice was considered correct if the mice entered an arm containing the food reward. Similarly, for spatial memory tasks, one arm out of eight was baited with a food reward, and various parameters were recorded.

Neuromuscular coordination tests

The neuromuscular coordination of mice was recorded by using two different methods; The rotarod, and wire hanging test. For both the tests, mice were trained for three consecutive days with three trials per day. The maximum time allowed on the rotarod or wire mesh during the experiment was 300 and 120 seconds respectively. The rotarod was initially set at a speed of 4 rpm at the start of the test and accelerated to 40 rpm over 300 seconds. The latency to fall from the rotarod or wire mesh was recorded for each mouse, and the mean latency to fall for each group was calculated.

mRNA isolation and sequencing

Total RNA was isolated from the brain's hippocampus region by using the TRI reagent (sigma T9424) according to the manufacturer's instructions. Briefly, 50–100 mg of brain tissue samples were homogenized in 1 ml of TRI reagent using a polytron homogenizer (PT 2500 E). The samples were incubated for five

minutes at room temperature, after that, 0.2 ml of chloroform per ml of TRI reagent was added and vortexed and incubated at RT for 10 minutes. The samples were centrifuged at 14,000g for 15 minutes at 4 °C, the upper aqueous phase containing RNA was collected and 2-propanol (0.5 ml per 1 ml of TRI reagent) was added and incubated at RT for the next 10 minutes. Further, centrifugation was done at 12,000 g for 10 minutes at 4 °C. The supernatants were discarded, and 75% ethanol (1 ml per 1 ml of TRI reagent used) was added to the resultant RNA precipitate pellet. The samples were sent to the Neuberg Centre for Genomic Medicine, Ahmedabad, India, for further processing and sequencing. According to them, the RNA quality was assessed by Qubit 4 Fluorometer (Thermofisher, Q33238) using an RNA High Sensitivity (HS) assay kit (Thermofisher, Q32852) following the manufacturer's instruction. All RNA samples with RNA Integrity Number (RIN) greater than 7.2 were used for library preparation. libraries were prepared with 25 ng of mRNA, poly(A)-selected from 5 µg total RNA, with 13 cycles of PCR amplification. Libraries were quantified by Qubit 4 Fluorometer using a DNA High Sensitivity assay kit (Thermofisher, cat no. Q32851) following the manufacturer's protocol. Library size was confirmed by Tapestation 4150 (Agilent) utilizing highly sensitive D1000 screentapes (Agilent, cat no. 5067- 5582) following manufacturers' protocol. Pooled library was loaded onto NOVASEQ 6000 high-output flow cell from Illumina (FC-404-2002), and 150 base pair pair-end sequencing was performed on a NOVASEQ 6000 sequencer. Libraries were sequenced to an average depth of 40 million reads per sample. Sequences were aligned to the M14 genome (protein coding, https://www.gencodegenes.org/mouse/release_M14.html) with STAR (v2.7.10a) and assigned to features with subread: feature Counts (v2.0.1). The raw data were processed by R statistical software (v 4.2.2, https://www.r-project.org/). The feature count data were annotated with org.Mm.eg.db (Annotation Dbi) to get the gene symbols. Gene IDs without gene annotation or with multiple gene symbols were removed. We got a total of 30951 genes after removing 55 duplicated genes.

Differential gene expression analysis

DESeq2 (v 1.38.1) package was used to analyze the differential gene expression. The total feature count of less than 5 in a gene's row was removed. Differential expression analysis was performed on the remaining 22096 genes. Regularized Log Transformation (RLT) was used to normalize the data. The unbiased approach was used for Principal Component Analysis (PCA) and to visualize the distribution of clusters after the crocetin treatment.

Hierarchical clustering of differentially expressed genes (DEGs)

Heatmap and hierarchical clustering were used to ensure the selected genes (up-regulated and down-regulated) were distinguished well between control and treated conditions.

Gene Ontology (GO) and Kyoto Encyclopedia of Genes and Genomes (KEGG) pathway enrichment analysis of differentially expressed genes.

GO and KEGG pathway enrichment analyses were performed using the clusterProfiler (v 4.6.0) and org.Hs.eg.db (3.16.0) packages.

SNP and Indels

Single Nucleotide Polymorphisms (SNPs) and DNA insertions and deletions (indels), were identified using Genome Analysis Tool Kit 4 (GATK4) (4.3.0.0). Sequences were aligned with grcm38 (https://www.gencodegenes.org/mouse/release_M14.html) with BWA-2 (0.7.17-r1188). Duplicates were marked by using GATK4 MarkDuplicatesSpark. Samtools (1.16.1) was used for sorting the mitochondrial genome. Picard, R (4.2.0) and Samtools were used for Collect Alignment & Insert Size Metrics. GATK4 was used for Variants calling, Extract SNPs & Indels, Filter SNPs and Indels, and Base Quality Score Recalibration (BQSR). Further vcf files were aligned and marked for SNP and Indels using the integrative genome viewer (IGV) software (2.16.0).

Liquid chromatography-mass spectrometry (LC-MS)

Mice brain tissue samples were isolated and immediately snap-frozen in liquid nitrogen. 50-100 mg of frozen

tissue samples were taken for further analysis. The samples were lysed in water: methanol (60: 40) solvent system, 0.5 ml solvent for 100 mg tissue using an ultrasonic homogenizer (sonics VCX750, 40% amplitude, 3 pulses of 7 sec each at 4°C). The samples were incubated at 4°C for 30 minutes with vertexing vigorously after every 10 minutes interval, followed by centrifugation at 14000g for 20 minutes at 4°C. The supernatant was collected, and a syringe filter was used to filter out any remaining debris or impurities. Samples were taken for further LCMS quantification of ATP, ADP, AMP, NAD+, and NADH. The remaining pellet was used to quantify the protein using the Bradford method, and the quantified metabolites were further normalized with total protein. The LCMS analysis conditions are listed in Table 1.

Western blotting

The hippocampi were isolated and snap frozen in liquid nitrogen. 20-30 mg of tissue were lysed in RIPA buffer followed by ultrasonic homogenization (sonics VCX750, 30% amplitude, 3 pulses of 7 sec each at 4°C). Samples were centrifuged at 14000 g for 20 minutes at 4°C and the supernatants were collected. A total of 40 µg protein was loaded onto an SDS-PAGE gel for separation and transfer to PVDF membrane. Blots were blocked by 5% non-fat dry milk for 1 hour and overnight incubation at 4 °C with anti-ND5, and anti-ND6 antibodies. Blots were further incubated with secondary antibody before ECL detection. The blots were quantified using ImageJ software.

Culturing and aging of primary Astrocyte

The 1-5-days old C57BL/6J mouse pups were used to culture the primary astrocytes. CO2 inhalation was used to euthanize, and the brains were collected in a sterile dish containing cold media. The meninges and blood vessels were removed from the brain, and brain tissue was transferred to a culture dish containing cold DMEM media. The brain tissue was cut into smaller pieces using sterile scissors, followed by 2-3 PBS washes. After that, brain tissue pieces were incubated for 20-25 minutes in a 0.25% trypsin-EDTA solution at 37 °C. The trypsin-EDTA solution was neutralized with 10% FBS-DMEM, and the cell suspension was centrifuged at 1000 rpm for 5 minutes. The supernatant was discarded, and the cell pellet was resuspended in complete DMEM followed by culture in humidified incubator at 37 °C with 5% CO2. After 48 h, the media containing non-adherent cells were replaced with fresh complete DMEM (Sigma-D5523). The media were changed every fourth day until the astrocytes were confluent and ready for subculture. The astrocytes were aged by serial passaging until the fourth passage.

Confocal Microscopy

The aged primary astrocytes were seeded in the optical bottom 96 well plate (Thermo-165305). Cells were treated with crocetin (25 µM) for 15 days, the media were changed every 4^{th} day until the 15^{th} day of treatment. Fresh media containing mitoTraker Red CMXRos (Invitrogen-M7512) and bis-benzamide was added to the cells after 15 days of treatment. After 30 min of incubation, images were captured using CQ1(Yokogawa) confocal quantitative Image Cytometer. Fifteen fields were captured from each treatment group at 40X magnification. More than 1500 cells from each group were taken for further analysis. The images were analyzed using cell pathfinder software.

Flow Cytometer

Similarly, for flow- cytometry analysis cells were seeded in 6- well plate. After 15 days of treatment with crocetin mitoTraker Red CMXRos was added 30 min before the flow cytometer-based analysis.

Statistical analysis

All the data of crocetin and control group except transcriptomic data were analyzed using a two-tailed unpaired t-test, and a p-value of less than 0.1 is considered statistically significant using the GraphPad Prism software (version 9.0.0 (121)), with statistical significance determined as $P < 0.05$ and checked for normal distribution. Outliers were excluded based on a Grubbs test with a value set at a 0.05 significance level. Transcriptomics data were analysed using R (4.2.0), with Log 2-fold change (LFC) >0.3 in the gene

expression significant at adjusted p-value <0.05. The categories significantly enriched (p-value < 0.05) were considered for GO and KEGG analysis.

Acknowledgments

This study was supported and financed by the Council of Scientific and Industrial Research (CSIR), India, through the project HCP-0038 (CSIR-Phytopharmaceutical Mission, phase-1 & 2). We are grateful to CSIR for providing Research Fellowships to Ms. Sushil Choudhary and DST for supporting the fellowship of Dr. Abhishek Gour. We are highly thankful to Dr. Manish Dutt for his help in solving the Python and r language codes. We appreciate the help rendered by Dr. Ravail Singh for his help in improving the presentation of Figures. We are also thankful to Dr. Pankaj Chhiber for helping us acquire hematological samples. We are also thankful to Dr. Ajay P. Gupta and Dr. Varun Pratap Singh for their help in standardizing the LCMS and HPLC protocols. This manuscript has been given institutional MS Number: CSIR-IIIM/IPR/00575.

Competing Interests

The authors declare no competing interests.

Data Availability Statement

The data that supports the findings of this study are available in the supplementary material of this article. However, the complete transcriptome sequencing data files have been uploaded on intuitional server, which can be accessed through the link provided in the cross-reference hyperlink document.

References

Ances BM, Liang CL, Leontiev O, Perthen JE, Fleisher AS, Lansing AE*, et al.* (2009). Effects of aging on cerebral blood flow, oxygen metabolism, and blood oxygenation level dependent responses to visual stimulation. Hum Brain Mapp 30**:** 1120-1132.

Arjun R, Acharya S, Shender BS, Rorres C, Hrebien L, & Kam M (2019). Correlation of Cognitive Scores and the Onset of Hypoxia. Aerosp Med Hum Perform 90**:** 429-439.

Borson S, Scanlan J, Friedman S, Zuhr E, Fields J, Aylward E*, et al.* (2008). Modeling the impact of COPD on the brain. Int J Chron Obstruct Pulmon Dis 3**:** 429-434.

Boveris A, & Navarro A (2008). Brain mitochondrial dysfunction in aging. IUBMB Life 60**:** 308-314.

Dodd JW, Getov SV, & Jones PW (2010). Cognitive function in COPD. Eur Respir J 35**:** 913-922.

Ferrari M, Jain IH, Goldberger O, Rezoagli E, Thoonen R, Cheng KH*, et al.* (2017). Hypoxia treatment reverses neurodegenerative disease in a mouse model of Leigh syndrome. Proc Natl Acad Sci U S A 114**:**E4241-E4250.

Fricker M, Tolkovsky AM, Borutaite V, Coleman M, & Brown GC (2018). Neuronal Cell Death. Physiol Rev 98**:** 813-880.

Gomes AP, Price NL, Ling AJ, Moslehi JJ, Montgomery MK, Rajman L*, et al.* (2013). Declining NAD(+) induces a pseudohypoxic state disrupting nuclear-mitochondrial communication during aging. Cell 155**:** 1624-1638.

Gorman AM (2008). Neuronal cell death in neurodegenerative diseases: recurring themes around protein handling. J Cell Mol Med 12**:**2263-2280.

Goyal MS, Vlassenko AG, Blazey TM, Su Y, Couture LE, Durbin TJ*, et al.* (2017). Loss of Brain Aerobic Glycolysis in Normal Human Aging. Cell Metab 26**:** 353-360 e353.

Guo J, Huang X, Dou L, Yan M, Shen T, Tang W*, et al.* (2022). Aging and aging-related diseases: from molecular mechanisms to interventions and treatments. Signal Transduct Target Ther 7**:**391.

Haghani A, Johnson RG, Woodward NC, Feinberg JI, Lewis K, Ladd-Acosta C*, et al.* (2020). Adult mouse hippocampal transcriptome changes associated with long-term behavioral and metabolic effects of gestational air pollution toxicity. Transl Psychiatry 10**:** 218.

Hannula DE, Tranel D, & Cohen NJ (2006). The long and the short of it: relational memory impairments in amnesia, even at short lags. J Neurosci 26**:** 8352-8359.

Hong CH, Falvey C, Harris TB, Simonsick EM, Satterfield S, Ferrucci L*, et al.* (2013). Anemia and risk of dementia in older adults: findings from the Health ABC study. Neurology 81**:** 528-533.

Johri A, & Beal MF (2012). Mitochondrial dysfunction in neurodegenerative diseases. J Pharmacol Exp Ther 342**:** 619-630.

Khakh BS, & Sofroniew MV (2015). Diversity of astrocyte functions and phenotypes in neural circuits. Nat Neurosci 18**:** 942-952.

Kim HJ, Park HK, Lim DW, Choi MH, Kim HJ, Lee IH*, et al.* (2013). Effects of oxygen concentration and flow rate on cognitive ability and physiological responses in the elderly. Neural Regen Res 8**:**264-269.

Kronenberg G, Gertz K, Schoner J, Bertram L, Liman T, Steinhagen-Thiessen E*, et al.* (2021). BDNF serum concentrations in 2053 participants of the Berlin Aging Study II. Neurobiol Aging 101**:** 221-223.

Leuner K, Hauptmann S, Abdel-Kader R, Scherping I, Keil U, Strosznajder JB*, et al.* (2007). Mitochondrial dysfunction: the first domino in brain aging and Alzheimer's disease? Antioxid Redox Signal 9**:**1659-1675.

Li G, Liu J, Guo M, Gu Y, Guan Y, Shao Q*, et al.* (2022). Chronic hypoxia leads to cognitive impairment by promoting HIF-2alpha-mediated ceramide catabolism and alpha-synuclein hyperphosphorylation. Cell Death Discov 8**:** 473.

Lowery EM, Brubaker AL, Kuhlmann E, & Kovacs EJ (2013). The aging lung. Clin Interv Aging 8**:** 1489-1496.

Mattson MP, & Arumugam TV (2018). Hallmarks of Brain Aging: Adaptive and Pathological Modification by Metabolic States. Cell Metab 27**:** 1176-1199.

Mitchell P (1970). Aspects of the chemiosmotic hypothesis. Biochem J 116**:** 5P-6P.

Moeini M, Lu X, Avti PK, Damseh R, Belanger S, Picard F*, et al.*(2018). Compromised microvascular oxygen delivery increases brain tissue vulnerability with age. Sci Rep 8**:** 8219.

Okonkwo DO, Wagner J, Melon DE, Alden T, Stone JR, Helm GA*, et al.* (2003). Trans-sodium crocetinate increases oxygen delivery to brain parenchyma in rats on oxygen supplementation. Neurosci Lett 352**:** 97-100.

Oruganty-Das A, Ng T, Udagawa T, Goh EL, & Richter JD (2012). Translational control of mitochondrial energy production mediates neuron morphogenesis. Cell Metab 16**:** 789-800.

Park CB, & Larsson NG (2011). Mitochondrial DNA mutations in disease and aging. The Journal of cell biology 193**:** 809-818.

Podyma B, Parekh K, Guler AD, & Deppmann CD (2021). Metabolic homeostasis via BDNF and its receptors. Trends Endocrinol Metab 32**:** 488-499.

Reddy CN, Bharate SB, Vishwakarma RA, & Bharate SS (2020). Chemical analysis of saffron by HPLC based crocetin estimation. Journal of pharmaceutical and biomedical analysis 181**:** 113094.

Shah HM, Jain AS, Joshi SV, & Kharkar PS (2021). Crocetin and related oxygen diffusion-enhancing compounds: Review of chemical synthesis, pharmacology, clinical development, and novel therapeutic applications. Drug Dev Res 82**:** 883-895.

Shapira R, Gdalyahu A, Gottfried I, Sasson E, Hadanny A, Efrati S, *et al.* (2021). Hyperbaric oxygen therapy alleviates vascular dysfunction and amyloid burden in an Alzheimer's disease mouse model and in elderly patients. Aging (Albany NY) 13**:** 20935-20961.

Snyder B, Simone SM, Giovannetti T, & Floyd TF (2021). Cerebral Hypoxia: Its Role in Age-Related Chronic and Acute Cognitive Dysfunction. Anesth Analg 132**:** 1502-1513.

Stennett AK, Dempsey GL, & Gainer JL (2006). trans-Sodium crocetinate and diffusion enhancement. J Phys Chem B 110**:** 18078-18080.

Tyshkovskiy A, Bozaykut P, Borodinova AA, Gerashchenko MV, Ables GP, Garratt M, *et al.* (2019). Identification and Application of Gene Expression Signatures Associated with Lifespan Extension. Cell Metab 30**:** 573-593 e578.

Verkhratsky A, & Nedergaard M (2018). Physiology of Astroglia. Physiol Rev 98**:** 239-389.

Vold ML, Aasebo U, Wilsgaard T, & Melbye H (2015). Low oxygen saturation and mortality in an adult cohort: the Tromso study. BMC Pulm Med 15**:** 9.

Wang Y, Schretter C, Clarke R, & Lee KS (2015). Perihematomal Cellular Injury Is Reduced by Trans-sodium Crocetinate in a Model of Intracerebral Hemorrhage. Mol Neurobiol 52**:** 985-989.

Wang Y, Yoshimura R, Manabe H, Schretter C, Clarke R, Cai Y, *et al.* (2014). Trans-sodium crocetinate improves outcomes in rodent models of occlusive and hemorrhagic stroke. Brain Res 1583**:** 245-254.

Wani A, Al Rihani SB, Sharma A, Weadick B, Govindarajan R, Khan SU, *et al.* (2021). Crocetin promotes clearance of amyloid-beta by inducing autophagy via the STK11/LKB1-mediated AMPK pathway. Autophagy 17**:** 3813-3832.

Webster NJ, Green KN, Settle VJ, Peers C, & Vaughan PF (2004). Altered processing of the amyloid precursor protein and decreased expression of ADAM 10 by chronic hypoxia in SH-SY5Y: no role for the stress-activated JNK and p38 signalling pathways. Brain Res Mol Brain Res 130**:**161-169.

Wilkins HM, & Swerdlow RH (2021). Mitochondrial links between brain aging and Alzheimer's disease. Transl Neurodegener 10**:** 33.

Wilson DM, 3rd, Cookson MR, Van Den Bosch L, Zetterberg H, Holtzman DM, & Dewachter I (2023). Hallmarks of neurodegenerative diseases. Cell 186**:** 693-714.

Yao J, Irwin RW, Zhao L, Nilsen J, Hamilton RT, & Brinton RD (2009). Mitochondrial bioenergetic deficit precedes Alzheimer's pathology in female mouse model of Alzheimer's disease. Proc Natl Acad Sci U S A 106**:** 14670-14675.

Legends to Figures

Figure 1. Old mice showed significant improvement in brain function after four months of chronic treatment with crocetin

(A) Brain pharmacokinetics of crocetin formulation after a single dose (10 mg kg^{-1}, n=5) and (B) after four months of dosing (10 mg kg^{-1}, n=8). The quantity of crocetin in the brain, even after four months of dosing (was comparable to single dosing when the brain samples were isolated after four h of dosing. (C) Analysis of spatial memory behavior was done by using a radial arm maze after four months of dosing in old mice (n=7), and the following parameters were checked; Mean latency to the baited arm, baited arm time, entries to non-baited arms, and distance travelled to search their reward (D) Analysis of working memory by using radial arm maze in mice (n=7), following parameters were tested; Latency to the first entry to the baited arm, baited arm time, non-baited arm time, and entries to the baited arm. (E) Open field test was done in both sets of animals used for working and spatial memory (n=14), the behavior parameters analyzed included; Distance travelled, time mobile, centre time, corner time, average speed, and the number of vertical movement count. Data here are shown as mean ± SEM. The statistical significance

was calculated by comparing the control and crocetin groups. The p-values were calculated using a two-tailed unpaired student-t test and are shown separately for each bar graph.

Figure 2. Analysis of differential gene expression in hippocampi of old mice after treatment with crocetin

Clustering of gene expression from hippocampi of mice. (A) Representation of gene expression in Principal Component (PC) space. Values in parenthesis indicate the percentage of variance explained by control (blue) and crocetin groups (red). (B) Volcano plot of genes from hippocampi of mice. The red dots represent significantly upregulated genes (115), and the blue dots show significantly downregulated genes (39). (C) Heat map of some of the representative genes, which were differentially upregulated in hippocampi of mice treated with crocetin in comparison to the control group (standardized expression level; red boxes represent high expression; blue boxes signify low expression (the complete list of differentially upregulated genes is given in the Supplementary Figure S3B). (D) Heat map of all the downregulated genes. (F) Heat map of all the upregulated genes of the mitochondrial genome in mice hippocampi. padj < 0.05 and $|\log2(\text{fold change})| > \log2(0.3)$ were considered to be statistically significant, n = 7 mice in each group.

Figure 3. Effect of Crocetin on electron transport chain in the brain cells of old mice

(A) Gene Ontology (GO) enrichment analyses of genes expression in hippocampi of control and crocetin-treated groups, all significant differentially expressed pathways are shown in the dot plot, categorized as BP (biological processes), CC (cellular component), and MF (molecular function). (B) KEGG pathway analysis of differentially expressed genes in hippocampi of control and crocetin groups. padj < 0.05 was determined to be significant for this analysis. LCMS-based quantification of (C) NAD^+ and NADH, (D) ATP and AMP, and (E) Glucose in the brain of mice from control and crocetin groups. Data are shown as mean ± SEM and statistical significance was calculated by comparing the control and crocetin groups. p-values were calculated using a two-tailed unpaired student-t test and are shown for each bar graph in the figure.

Figure 4. Crocetin treatment changed the hippocampi gene profile of old mice to bring it closer to young untreated mice

(A) Hierarchical clustering of gene expression tree of the normalized count of young (n=5), old (n=7), and crocetin (n=7) group (B) Normalized count of mitochondrial genome-specific genes ND1, ND2, ND3, ND4, ND5, and ND6 and Normalized count of nuclear genome-specific genes Bdnf, Uqcrq, Gfpt1, Eno3, Gabbar2, and Drosha. (D) Comparison of expression of ND5 and ND6 among young untreated, old untreated and old mice treated with crocetin through western blotting. The adjusted p-value < 0.05 was used to identify the genes, which were differentially upregulated in old treated mice and formed clusters closer to young mice. Data presented in Figure 4C are mean ± SEM, and statistical comparisons were made among the groups of young untreated, old untreated, and old mice treated with crocetin. p-values were calculated using a two-tailed unpaired student-t test and are shown for each bar graph.

Figure 5. Aged primary astrocytes showed improved mitochondrial function after treatment with crocetin

(A) Flow-cytometry analysis of mitochondrial membrane potential with mitoTraker Red CMXRos (B) Confocal analysis of mitochondrial membrane potential with mitoTraker Red CMXRos, Mean Fluorescence Intensity (MFI) was calculated for individual mitochondrion by using CellPathfinder software (C) Western blot analysis for ND5 and ND6 after 15 days treatment of aged primary astrocytes. The blot quantification was done using ImageJ software, and data were normalized with ACTB. (D) Quantification of energy metabolites NAD^+, NADH, ATP, and AMP in aged astrocytes by using LCMS. Data are Mean ± SEM, and p-values were calculated by using a two-tailed unpaired student-t test and are shown for each bar graph.

Figure 6. Crocetin upregulated the energy levels of other vital organs of the body and enhanced the median life span of male mice.

Quantification of energy metabolites NAD^+, NADH, ATP, and AMP in vital organs i.e., (A) Lung, (B) liver,

(C) Heart, and (D) Kidney by using LC-MS/MS method. (E) OGTT, after administration of glucose 1g kg^{-1} orally, the level of glucose was measured in the blood at different time points (F) Neuromuscular coordination was studied by examining latency to fall from an accelerating rod in the rotarod test (G) or elevated wire mesh in the wire hanging test (n=14) Data are shown as mean ± SEM and statistical significance was calculated by comparing the control and crocetin groups. p-values were calculated using a two-tailed unpaired student-t test and are shown separately for each bar graph. (H) Survival curves comparing control to crocetin-treated male mice (n=23). The p-values reflect outcome of log-rank (Mantel-Cox) test. The arrows at 480 days indicate the age at which crocetin treatment was initiated.

Legends to Tables

Table 1 . Chemicals, reagents, antibodies and other materials used in the study

Table 2 . LCMS/MS protocol conditions used to analyze energy metabolites.

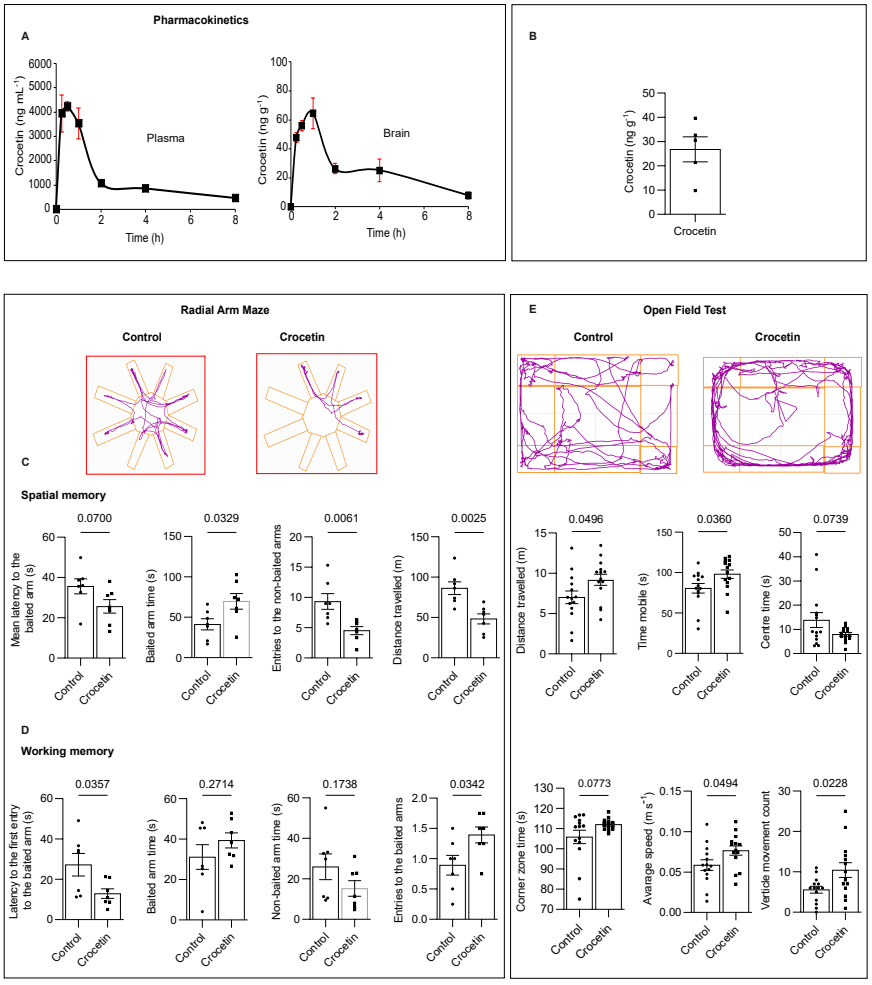

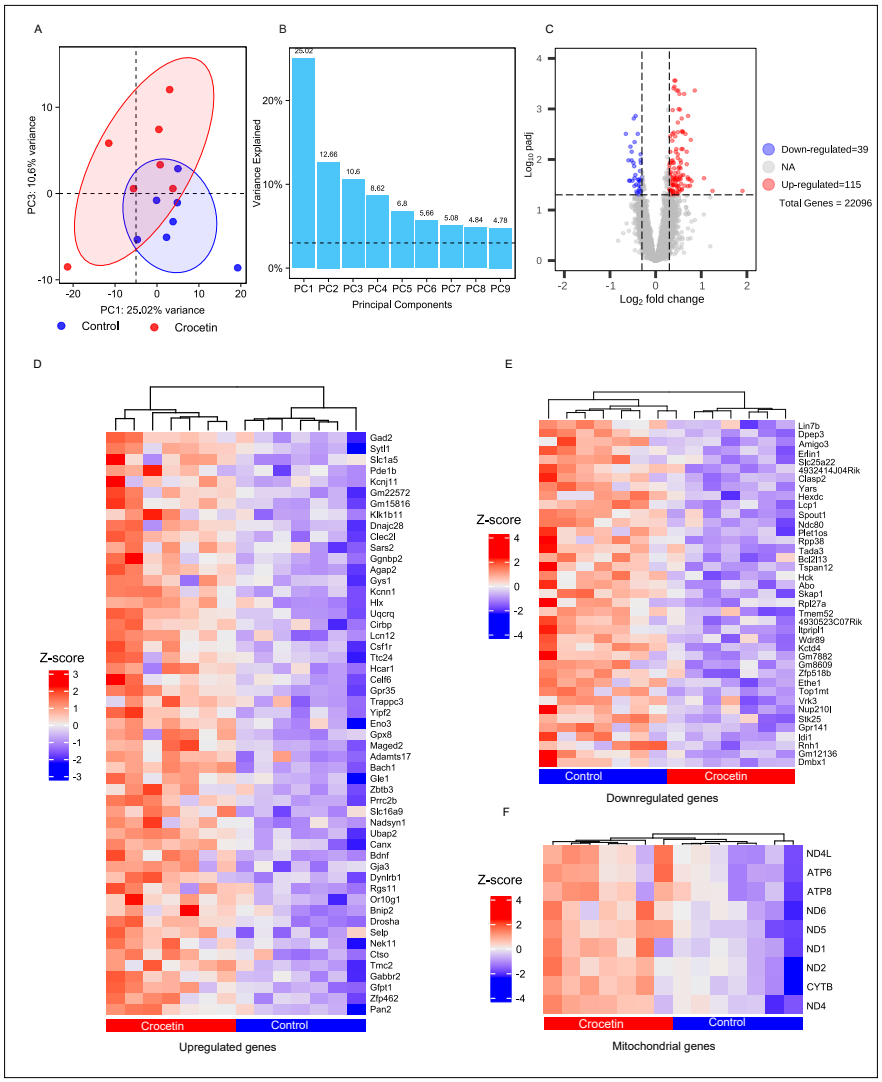

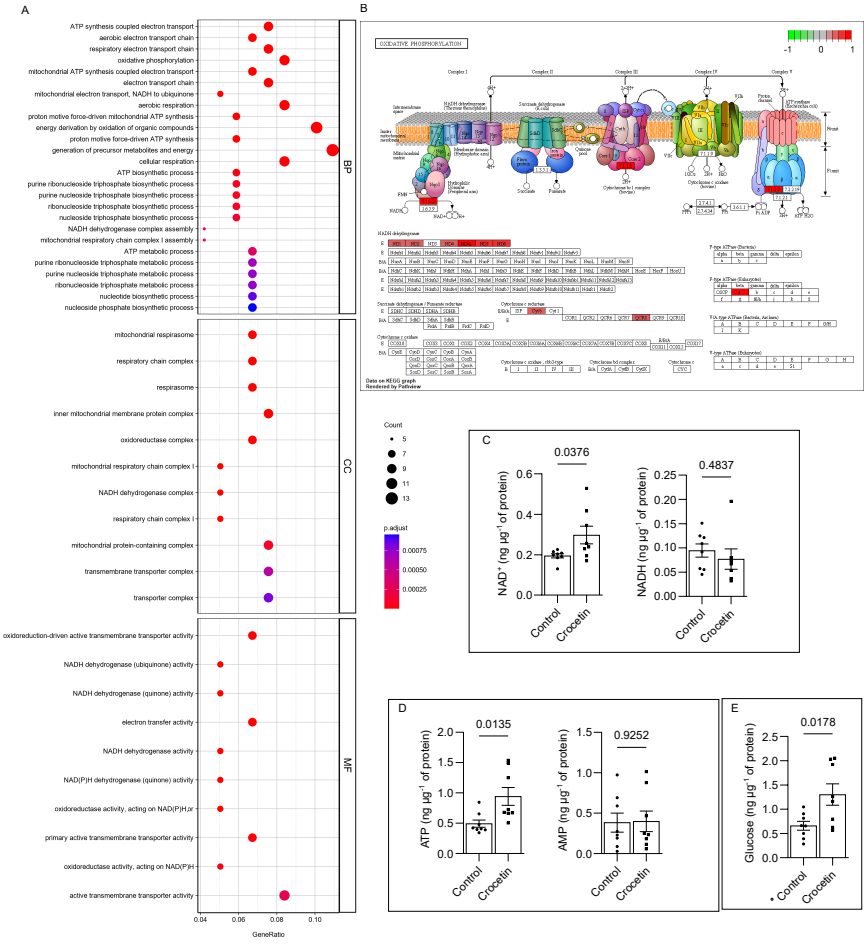

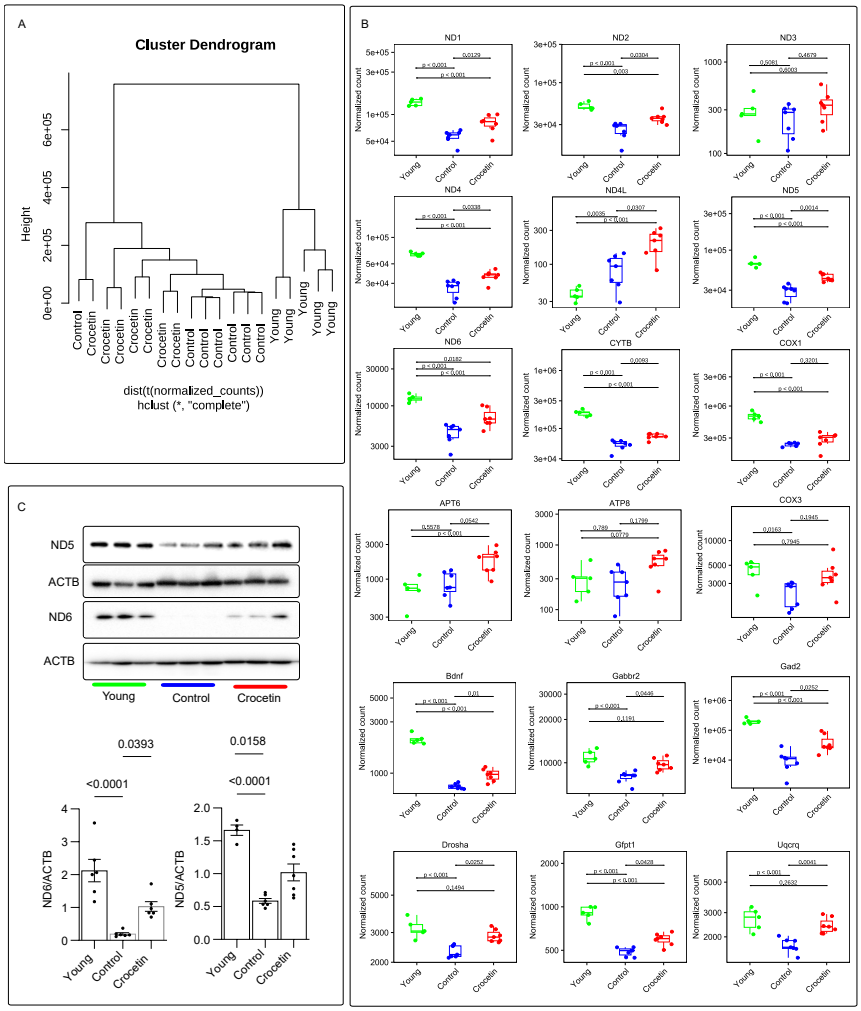

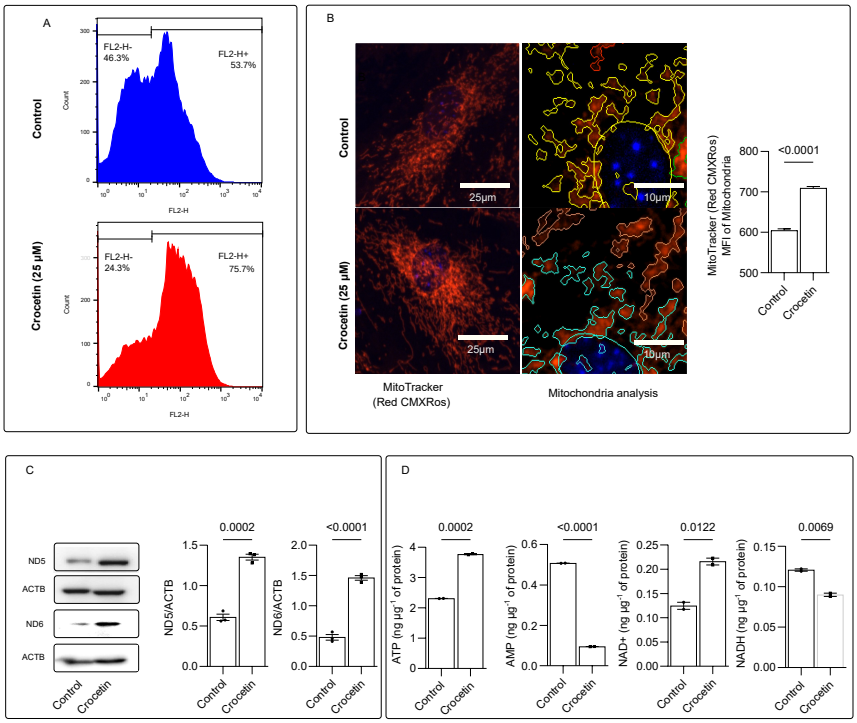

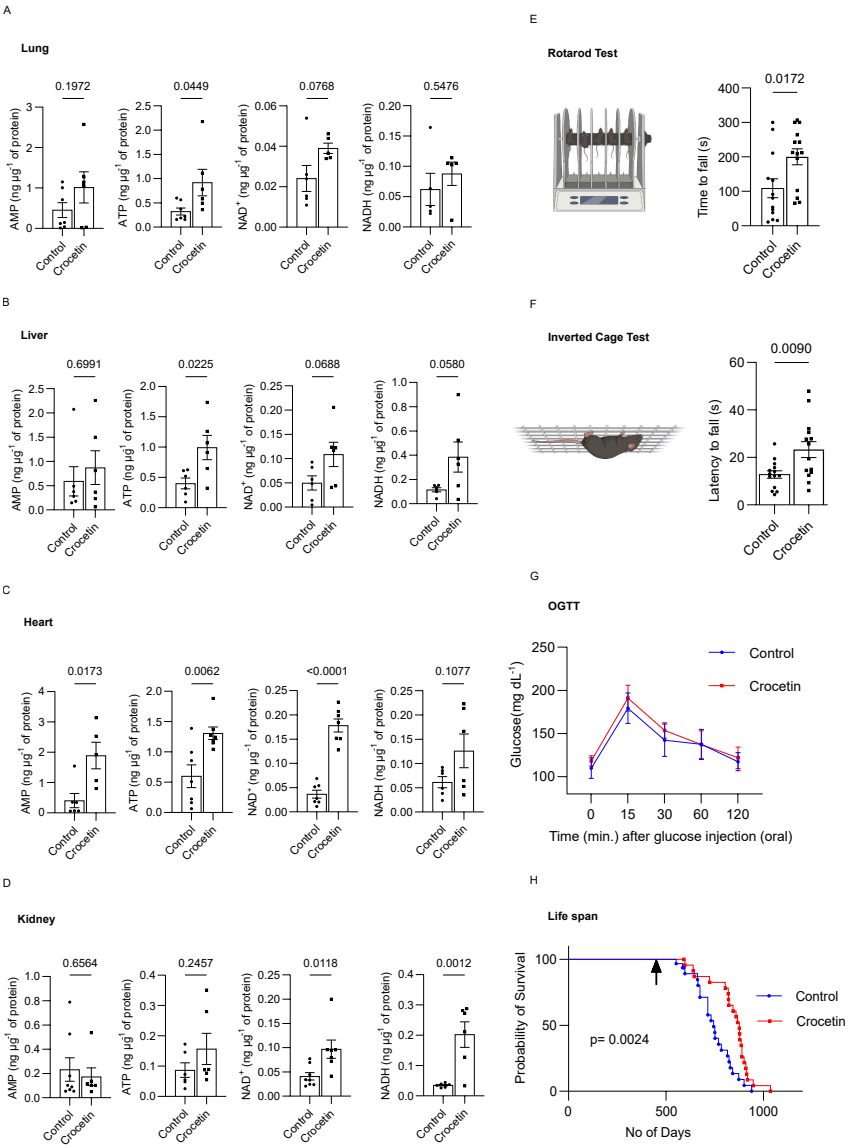

Hosted file

Table 1.docx available at https://authorea.com/users/671003/articles/670732-crocetin-delays-brain-and-body-aging-by-increasing-cellular-energy-levels-and-enhances-the-median-life-span-in-aged-c57bl-6j-mice

Hosted file

Table 2.docx available at https://authorea.com/users/671003/articles/670732-crocetin-delays-brain-and-body-aging-by-increasing-cellular-energy-levels-and-enhances-the-median-life-span-in-aged-c57bl-6j-mice